

## Search for a 33.9 MeV/ $c^2$ Neutral Particle in Pion Decay

J. A. Formaggio<sup>2</sup>, E. D. Zimmerman<sup>2</sup>, T. Adams<sup>4</sup>, A. Alton<sup>4</sup>, S. Avvakumov<sup>7</sup>, L. de Barbaro<sup>5</sup>, P. de Barbaro<sup>7</sup>, R. H. Bernstein<sup>3</sup>, A. Bodek<sup>7</sup>, T. Bolton<sup>4</sup>, J. Brau<sup>6</sup>, D. Buchholz<sup>5</sup>, H. Budd<sup>7</sup>, L. Bugel<sup>3</sup>, S. Case<sup>2</sup>, J. M. Conrad<sup>2</sup>, R. B. Drucker<sup>6</sup>, B. T. Fleming<sup>2</sup>, R. Frey<sup>6</sup>, J. Goldman<sup>4</sup>, M. Goncharov<sup>4</sup>, D. A. Harris<sup>7</sup>, R. A. Johnson<sup>1</sup>, J. H. Kim<sup>2</sup>, S. Koutsoliotas<sup>2</sup>, M. J. Lamm<sup>3</sup>, W. Marsh<sup>3</sup>, D. Mason<sup>6</sup>, K. S. McFarland<sup>7,3</sup>, C. McNulty<sup>2</sup>, D. Naples<sup>4</sup>, P. Nienaber<sup>3</sup>, A. Romosan<sup>2</sup>, W. K. Sakumoto<sup>7</sup>, H. M. Schellman<sup>5</sup>, M. H. Shaevitz<sup>2</sup>, P. Spentzouris<sup>2,3</sup>, E. G. Stern<sup>2</sup>, M. Vakili<sup>1</sup>, A. Vaitaitis<sup>2</sup>, V. Wu<sup>1</sup>, U. K. Yang<sup>7</sup>, J. Yu<sup>3</sup>, and G. P. Zeller<sup>5</sup>

<sup>1</sup> *University of Cincinnati, Cincinnati, OH 45221*

<sup>2</sup> *Columbia University, New York, NY 10027*

<sup>3</sup> *Fermilab, Batavia, IL 60510*

<sup>4</sup> *Kansas State University, Manhattan, KS 66506*

<sup>5</sup> *Northwestern University, Evanston, IL 97403*

<sup>6</sup> *University of Oregon, Eugene, OR 97403*

<sup>7</sup> *University of Rochester, Rochester, NY 14627*

(November 1, 2018)

The E815 (NuTeV) neutrino experiment has performed a search for a 33.9 MeV/ $c^2$  weakly-interacting neutral particle produced in pion decay. Such a particle may be responsible for an anomaly in the timing distribution of neutrino interactions in the KARMEN experiment. E815 has searched for this particle's decays in an instrumented decay region; no evidence for this particle was found. The search is sensitive to pion branching ratios as low as  $10^{-13}$ .

PACS numbers:14.80.-j, 12.60.-i, 13.20.Cz, 13.35.Hb

The KARMEN collaboration at the ISIS spallation neutron facility at the Rutherford Appleton Laboratory uses a pulsed neutrino beam resulting from stopped pion and muon decays to study neutrino-nucleon interactions. Their experiment has reported an anomaly in the timing distribution of neutrino interactions from stopped muon decays [1]. One possible explanation for the anomaly is an exotic pion decay, where a neutral weakly-interacting or sterile particle is produced and travels 17.7 m to the KARMEN detector with a velocity of 4.9 m/ $\mu$ s. Upon reaching the KARMEN detector, the exotic particle decays to a partially electromagnetic state, such as  $e^+e^-\nu$  or  $\gamma\nu$ . The  $e^+e^-\nu$  decay is strongly favored by recent KARMEN data [2]. This slow moving exotic particle (hereafter denoted as  $Q^0$ ) would have a mass of 33.9 MeV/ $c^2$ , which is near the kinematic threshold for pion decay.

The KARMEN experiment reports a signal curve for pion branching ratio  $B(\pi \rightarrow \mu + Q^0) \cdot B(Q^0 \rightarrow \text{visible})$  versus lifetime. Their signal region extends as low as  $10^{-16}$  for a lifetime of 3.6  $\mu$ s. For branching ratios above this minimum, there exist two solutions to the KARMEN anomaly (at small and large lifetimes). Certain portions of the KARMEN signal have already been excluded. Experiments at PSI [3,4] have performed searches for this exotic particle by studying the momentum spectrum of muons and electrons produced by  $\pi^+$  decays in flight. PSI has excluded any exotic pion decays to muons with branching ratios above  $2.1 \times 10^{-8}$  at 90% C.L., and to electrons with branching ratios above  $0.9 \times 10^{-6}$  at 90% C.L. In addition, there exist astrophysical constraints on

certain decay modes of the  $Q^0$  which exclude lifetimes above  $10^3$  s [5]. Despite the above limits, portions of the KARMEN allowed signal region remain to be addressed.

The E815 (NuTeV) neutrino experiment at Fermilab has performed a direct search for the  $Q^0$  decay by combining the capabilities of a high intensity neutrino beam with an instrumented decay region (the “decay channel”). During the 1996-1997 fixed target run at Fermilab, NuTeV received  $2.54 \times 10^{18}$  800 GeV protons striking a BeO target with the detector configured for this search. The secondary pions and kaons produced from the interaction were subsequently sign-selected using a series of magnets and focused down a beamline at a 7.8 mrad angle from the primary proton beam direction. The pions and kaons could then decay in a 440 m pipe before hitting a beam dump. A total of  $(1.4 \pm 0.1) \times 10^{15}$  pion decays and  $(3.6 \pm 0.4) \times 10^{14}$  kaon decays occurred in the pipe. The neutral weakly-interacting decay products (neutrinos and possibly  $Q^0$ 's) traveled through approximately 900 meters of earth berm shielding before arriving at the decay channel.

The instrumented decay channel consisted of a series of helium bags, extending a total of 34 meters in length, interspersed with 3 m  $\times$  3 m multi-wire argon-ethane drift chambers. The drift chambers were designed to track charged particles from decays occurring within the helium. Upstream of the decay channel stood a 4.6 m  $\times$  4.6 m array of scintillation plates, known as the veto wall, used to detect any charged particles entering from upstream of the detector. Downstream of the decay channel was the Lab E neutrino detector, which consisted

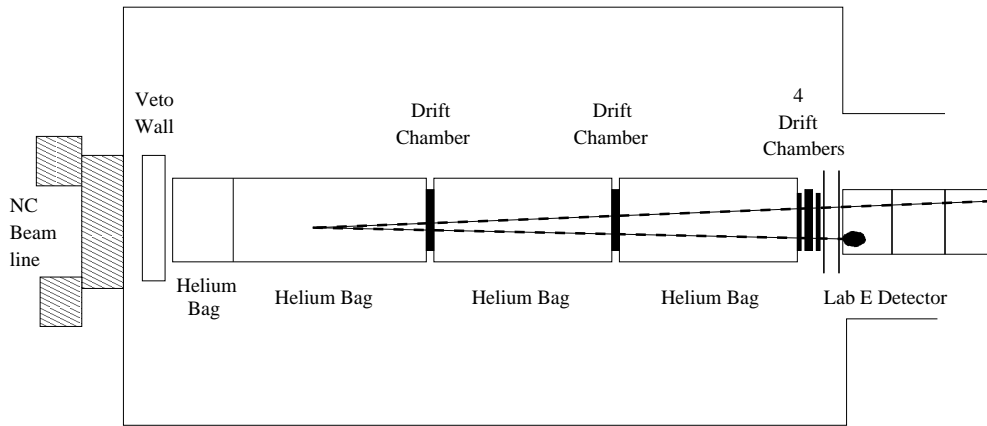


FIG. 1. Schematic of the NuTeV decay channel, including the veto wall, helium bags, drift chambers, and calorimeter.

of a 690-ton iron-scintillator sampling calorimeter interspersed with drift chambers. The Lab E detector provided triggering, energy measurement, and final particle identification for tracks entering from the decay channel. Particles were identified by their penetration into the calorimeter: a muon produced a long track, a pion produced an elongated cluster of hits, and an electron or photon produced a compact cluster. More details of the decay channel and the calorimeter can be found elsewhere [6,7].

The decay channel was employed to search for the decay of the  $Q^0$ . The experimental signature of this decay is a low-mass, low-transverse momentum electron-positron pair having a vertex within the fiducial volume of the decay channel.

A series of analysis cuts isolated the  $Q^0$  from background. The cuts were divided into two categories: reconstruction and kinematic. Reconstruction cuts isolated two track events occurring within the fiducial volume of the decay channel. We required that two charged tracks originated from a common vertex, with no additional tracks associated with the vertex. By removing events with activity in the veto wall, we ensured that no charged tracks entered from upstream of the decay channel. We also required that each track had a small slope ( $< 10$  mr) relative to the beam axis; and that, when projected upstream to the veto wall, it fell within  $50''$  of the beam center. These cuts removed both cosmic rays and photons from neutrino interactions in the upstream berm. Finally, we required that each track be identified as an electron based on the shower shape in the calorimeter. Because of the small opening angle of the two tracks, the two electron showers manifested themselves as a single merged electron-like cluster within the calorimeter. The efficiency for identifying such an event as an  $ee$  pair was estimated from Monte Carlo studies to be 90.1%. The cluster energy was divided between the tracks based on a fit to the amount of multiple scattering each track underwent in the decay channel.

Because of its low mass, the  $Q^0$  possesses unique kinematic features which can be used to distinguish it from potential background sources, such as photons and deep-inelastic neutrino interactions. We have used effective scaling variables to represent the kinematics of the reconstructed events. The effective scaling variables  $x_{\text{eff}}$  and  $W_{\text{eff}}$  were calculated for each event using the following assumptions: 1) the event was a charged current neutrino interaction ( $\nu_\ell N \rightarrow \ell N' X$ ) and 2) the missing transverse momentum in the event was carried by an undetected final state nucleon. We have defined  $x_{\text{eff}} \equiv \frac{Q_{\text{vis}}^2}{2m_p \nu_{\text{vis}}}$  and  $W_{\text{eff}} \equiv \sqrt{m_p^2 + 2m_p \nu_{\text{vis}}/c^2 - Q_{\text{vis}}^2/c^2}$ , where  $Q_{\text{vis}}$  is the visible reconstructed 4-momentum transfer,  $\nu_{\text{vis}}$  is the reconstructed hadron (or electron) energy, and  $m_p$  is the proton mass. Using the above definitions, we required that all reconstructed events have  $x_{\text{eff}} < 0.001$  and  $W_{\text{eff}} > 2.5$  GeV/ $c^2$ . In addition, we required that the reconstructed transverse mass  $m_T$  ( $m_T \equiv |p_T| + \sqrt{p_T^2 + m_V^2}$ , where  $m_V$  is the invariant mass of the two charged tracks and  $p_T$  is the momentum transverse to the beam axis) be less than 250 MeV/ $c^2$ . Finally, we required that the total energy deposited by the  $e^+e^-$  pair be greater than 15 GeV. The effect of these cuts when applied to signal and typical background kinematic distributions can be seen in Figure 2. The total acceptance for  $Q^0$  events in the fiducial region was 15.6%.

The principal backgrounds originated from three main sources: neutrino interactions in the helium, neutrino interactions in the drift chambers, and neutral particles (mainly photons and kaons) from neutrino interactions in the berm and veto wall. Note that because the two electron tracks had a very small opening angle, the longitudinal vertex position resolution was quite poor ( $\sigma \approx 7$  m). Thus, interactions in the chambers could not be removed using a vertex position cut. We used the Lund Monte Carlo program [8] to simulate the  $\nu p$  deep-inelastic interactions in both the berm and the decay channel. Separate Monte Carlo programs were used to simulate hadronic resonance and diffractive single pion produc-

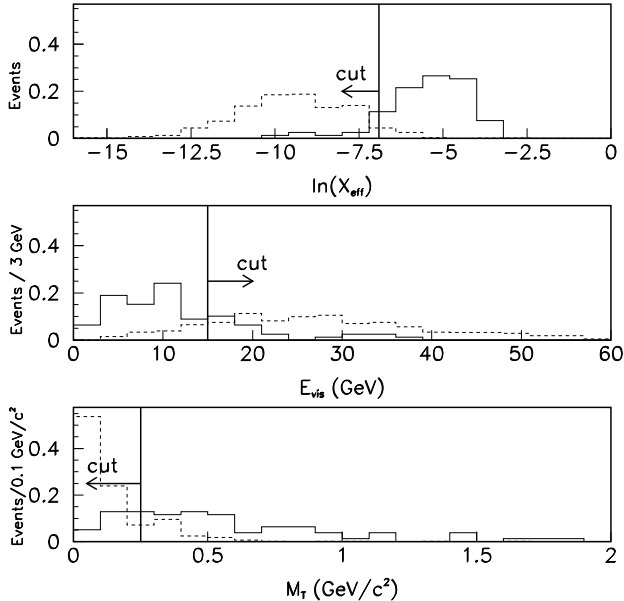


FIG. 2. Kinematic Monte Carlo distributions of  $x_{\text{eff}}$ , visible energy, and transverse mass for neutrino interactions (solid) and  $Q^0$  (dashed). All events shown have passed reconstruction cuts only and are relatively normalized.

tion [9,10]. The GEANT Monte Carlo program (version 3.21) [11] was used to simulate the decay channel and Lab E calorimeter. Based on our Monte Carlo study, we expected  $0.06 \pm 0.05$  total background events within our signal region (See Table I). The uncertainty on this background estimate is dominated by Monte Carlo statistics.

A blind analysis was performed. The signal region was hidden while cuts were developed based on Monte Carlo studies of signal efficiencies and background rejection. Before examining the data near or in the signal region, we performed a series of studies to verify our background estimates. Using the Monte Carlo, we made predictions for the following three quantities: 1) the number of low energy (below 15 GeV) and high transverse mass (above

TABLE I. Total Expected Background Events. Errors reflect Monte Carlo statistics.

Source	Rate
Photons	$0.04^{+0.02}_{-0.04}$
Kaons	$\ll 0.001$
Deep Inelastic Charged Current	$0.00 \pm 0.04$
Deep Inelastic Neutral Current	$0.02 \pm 0.02$
Cosmic rays	$\ll 0.001$
Quasi-Elastic Charged Current	$0.000 \pm 0.008$
Resonance Neutral Current	$0.000 \pm 0.003$
Diffractive Pions	$\pm 0.01$
Total	$0.06 \pm 0.05$

TABLE II. Background Study Results. Uncertainties are systematic.

Type of Event	Events Predicted	Events Seen
High Transverse Mass	$2.0 \pm 0.3$	1
$\mu\pi$ Events	$4.1 \pm 0.6$	3
Multiple Track Events	$13.7 \pm 1.8$	10

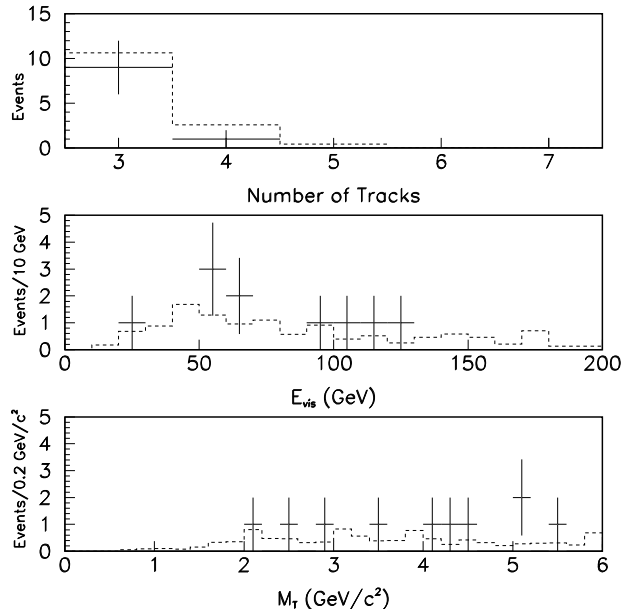


FIG. 3. Kinematic distributions of multiplicity, energy, and transverse mass for data (crosses) and background Monte Carlo (dashed) multi-track events. Monte Carlo is absolutely normalized.

500 MeV/ $c^2$ ) background events; 2) the number of  $\mu\pi$  events; and 3) the number of multi-track events occurring within our decay channel. The results of these studies (shown in Table II) demonstrate good agreement between data and the Monte Carlo predictions. In the case of multi-track events, where a larger sample of events was available, there was also good agreement for various kinematic distributions (see Figure 3).

The above acceptance estimate was based on a heavy neutrino model where the  $Q^0$  decays to  $e\nu$  [12]. We also considered additional decay models where the  $Q^0$  decays to  $\gamma\nu$  and  $\gamma\gamma\nu$ . The acceptances under these decay scenarios were  $(0.5 \pm 0.1)\%$  and  $(1.1 \pm 0.1)\%$ , respectively. The low efficiencies are due to the requirement that two tracks be reconstructed; this was only possible if a photon converted in the low-mass decay region before entering the calorimeter.

Systematic errors for this result were dominated by uncertainties on the number of pion decays in the pipe (6.8%) and the overall normalization. The sensitivity normalization was taken from a measurement of the number of neutrino interactions in the decay channel using

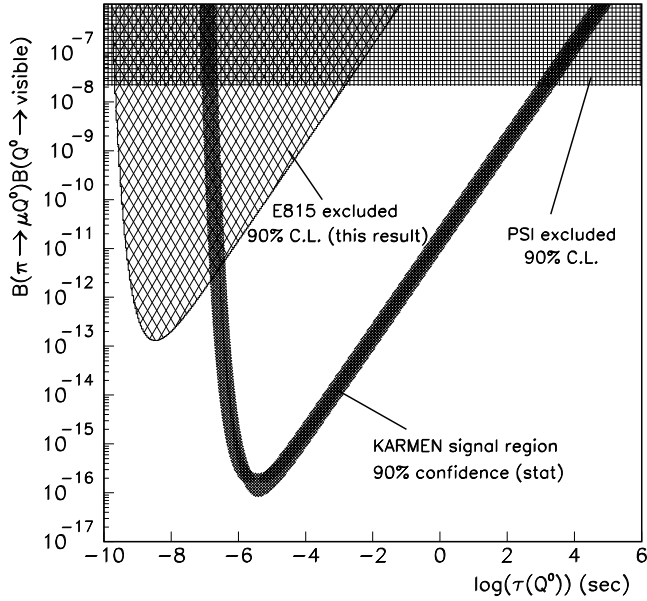


FIG. 4. Branching ratio versus lifetime plot for the Karmen signal and the exclusion regions (90% C.L.) from the NuTeV and PSI experiments. Systematic errors (except for decay model) have been included.

very loose cuts. This number was  $(10.0 \pm 4.3)\%$  below a prediction normalized to the number of neutrino interactions in the calorimeter. Considering this disagreement as a systematic error on the normalization, we have calculated a total systematic error of 12.1% on the sensitivity.

Upon analyzing the signal region, we found no events which passed the selection criteria. The probability of seeing zero events from an expected background of  $0.06 \pm 0.05$  is 94%. We thus present an upper limit, shown in Fig. 4, on  $B(\pi \rightarrow \mu + Q^0) \cdot B(Q^0 \rightarrow \text{visible})$ .<sup>\*</sup> NuTeV is also sensitive to  $\pi \rightarrow e + Q^0$ ; the limit is shown in Fig. 5.

This result excludes a region of parameter space which extends as low as four orders of magnitude below current limits on the short lifetime solution to the KARMEN anomaly. An experiment with significantly more pion decays will be necessary to confirm or rule out the longer lifetime and lower branching ratio regions.

This research was supported by the U.S. Department of

<sup>\*</sup> A simple interpretation of the  $Q^0$  is that the particle is a sterile heavy neutrino which mixes with the muon neutrino. This requires a branching ratio  $B(\pi \rightarrow \mu + Q^0) \approx 6 \times 10^{-8}$ , which has already been ruled out by the PSI limit [13]. Still viable is a model where the heavy neutrino is produced by a smaller mixing with  $\nu_\mu$  and decays primarily via a larger mixing with  $\nu_\tau$ , such that  $|\langle Q^0 | \nu_\mu \rangle| \cdot |\langle Q^0 | \nu_\tau \rangle| \approx 2 \times 10^{-6}$ . Within this model, we set a limit on this product  $|\langle Q^0 | \nu_\mu \rangle| \cdot |\langle Q^0 | \nu_\tau \rangle| < 1.4 \times 10^{-3}$  at 90% C.L.

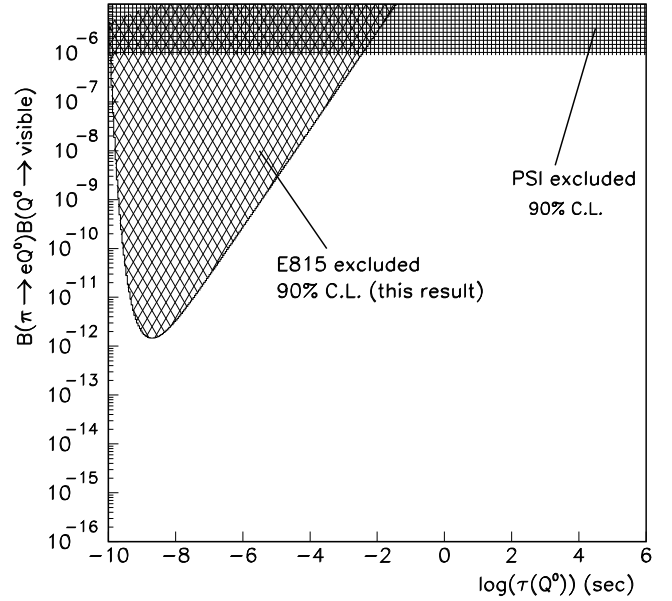


FIG. 5. Branching ratio versus lifetime plot for the NuTeV limit for  $\pi \rightarrow e + Q^0$ . Systematic errors (except for decay model) have been included.

Energy and the National Science Foundation. We thank the staff of FNAL for their contributions to the construction and support of this experiment during the 1996-1997 fixed target run.

---

[1] B. Zeitnitz, in Proc. 17th International Workshop on Weak Interactions and Neutrinos (1999).  
[2] C. Oehler, in Proc. Sixth Topical Seminar on Neutrino and Astroparticle Physics (1999).  
[3] M. Daum *et al.*, Phys. Lett. **B361**, 179 (1995).  
[4] N. De Leener-Rosier *et al.*, Phys. Lett. **D43**, 3611 (1991).  
[5] D. Choudhury *et al.*, e-print hep-ph/9911365.  
[6] A. Vaitaitis *et al.*, Phys. Rev. Lett. **83**, 4943 (1999).  
[7] D. A. Harris *et al.*, e-print hep-ex/9908056.  
[8] G. Ingelman *et al.*, Comput. Phys. Commun. **101**, 108 (1997).  
[9] D.Rein and L.M. Sehgal, Ann. Phys. **133**, 71 (1981).  
[10] T. Adams *et al.*, e-print hep-ex/9909041.  
[11] CERN CN/ASD, GEANT detector description and simulation library (1998).  
[12] M.Gronau, C.N. Leung, and J.L. Rosner, Phys. Rev. **D29**, 2539 (1984).  
[13] J. Govaerts, J. Deutsch, and P.M. Van Hove, Phys. Lett. **B389**, 700 (1996).